

Surface structures of normal paraffins and cyclohexane monolayers and thin crystals grown on the (111) crystal face of platinum. A low-energy electron diffraction study

Cite as: J. Chem. Phys. **66**, 2901 (1977); <https://doi.org/10.1063/1.434360>

Published Online: 26 August 2008

L. E. Firment, and G. A. Somorjai



View Online



Export Citation

ARTICLES YOU MAY BE INTERESTED IN

[Low-energy electron diffraction study of the surface of thin crystals and monolayers of normal paraffins and cyclohexane on the Ag\(111\) crystal surface](#)

The Journal of Chemical Physics **69**, 3940 (1978); <https://doi.org/10.1063/1.437132>

[Low-Energy Electron-Diffraction Study of the Clean \(100\), \(111\), and \(110\) Faces of Platinum](#)

The Journal of Chemical Physics **46**, 2539 (1967); <https://doi.org/10.1063/1.1841082>

[n-alkanes on Pt\(111\) and on C\(0001\)/Pt\(111\): Chain length dependence of kinetic desorption parameters](#)

The Journal of Chemical Physics **125**, 234308 (2006); <https://doi.org/10.1063/1.2400235>

PHYSICS TODAY
WHITEPAPERS

ADVANCED LIGHT CURE ADHESIVES

Take a closer look at what these environmentally friendly adhesive systems can do

READ NOW

PRESENTED BY
MASTERBOND
ADHESIVES | SEALANTS | COATINGS



Surface structures of normal paraffins and cyclohexane monolayers and thin crystals grown on the (111) crystal face of platinum. A low-energy electron diffraction study

L. E. Firment and G. A. Somorjai

Materials and Molecular Research Division, Lawrence Berkeley Laboratory, and Department of Chemistry, University of California, Berkeley, California 94720
(Received 23 September 1976)

The surfaces of the normal paraffins (C_3 – C_8) and cyclohexane have been studied using low-energy electron diffraction (LEED). The samples were prepared by vapor deposition on the (111) face of a platinum single crystal in ultrahigh vacuum, and were studied both as thick films and as adsorbed monolayers. These molecules form ordered monolayers on the clean metal surface in the temperature range 100–220 K and at a vapor flux corresponding to 10^{-7} Torr. In the adsorbed monolayers of the normal paraffins (C_4 – C_8), the molecules lie with their chain axes parallel to the Pt surface and Pt[1 $\bar{1}$ 0]. The paraffin monolayer structures undergo order–disorder transitions as a function of temperature. Multilayers condensed upon the ordered monolayers maintained the same orientation and packing as found in the monolayers. The surface structures of the growing organic crystals do not correspond to planes in their reported bulk crystal structures and are evidence for epitaxial growth of pseudomorphic crystal forms. Multilayers of *n*-octane and *n*-heptane condensed upon disordered monolayers have also grown with the (001) plane of the triclinic bulk crystal structures parallel to the surface. *n*-Butane has three monolayer structures on Pt(111) and one of the three is maintained during growth of the crystal. Cyclohexane forms an ordered monolayer, upon which a multilayer of cyclohexane grows exhibiting the (001) surface orientation of the monoclinic bulk crystal structure. Surface structures of saturated hydrocarbons are found to be very susceptible to electron beam induced damage. Surface charging interferes with LEED only at sample thicknesses greater than 200 Å.

INTRODUCTION

Recent studies of the surface structures of naphthalene and ice crystals by LEED¹ have shown that molecular crystal surfaces can indeed be studied by this technique. The experimental difficulties associated with using ultrahigh vacuum, growing the crystals *in situ* on suitable metal single crystal substrates, and the electron beam induced chemical and structural damage, can all be overcome. It appears that LEED can be used to study the surface structure of organic solids of technological and/or biological importance. The technique permits one to investigate the adsorbed monolayer structure, the surface morphology of the growing organic layer throughout the growth, and the surface structure of crystalline films of 200–2000 Å maximum thickness.

Using this method we have embarked on the investigation of the surface structure of organic crystals of varying size and/or chemical bonding. In this paper we report on the surface structures of saturated straight chain hydrocarbons (C_3 – C_8) and of cyclohexane, all grown from the vapor on a platinum (111) single crystal surface in the temperature range of 90–160 K.

Both monolayer and multilayer surface structures of the C_4 – C_8 hydrocarbons were ordered and from the unit cell size and orientation with respect to the platinum substrate, the packing of the molecules in the ordered domains has been determined. Although the diffraction beam intensities have been utilized recently to solve the surface structure of acetylene monolayer on the same Pt(111) surface used in this study,² the analysis of the LEED beam intensities has not been attempted for the molecular crystal surfaces. Instead, the trends observed in the unit mesh size and orientation for the en-

tire series of *n*-paraffins have been used to identify the surface structures of molecules in the monolayer and in the surface of the molecular crystals. The paraffin molecules lie with their chains parallel to the platinum surface in the monolayer and their packing and orientation remain unchanged during the crystal growth. Similarities between LEED data and the reported cyclohexane crystal structure support a model in which monolayers of cyclohexane are adsorbed with the molecules approximately parallel to the Pt substrate. The adsorbed C_3 – C_8 hydrocarbons undergo surface order–disorder transformations as a function of temperature. The rate of electron beam damage for saturated hydrocarbon crystal surfaces is greater than for conjugated unsaturated hydrocarbon systems.

EXPERIMENTAL

The experiments were performed in an ion-pumped Varian LEED apparatus fitted with a liquid nitrogen cooled sample manipulator. The apparatus, Pt(111) crystal preparations, and general procedures were described in the previous paper.¹

The hydrocarbon samples were grown as vapor deposited films upon the Pt substrate. The vapor was admitted to the chamber through a needle 1.5 cm from the crystal face. Film thickness and vapor flux were calibrated using an optical interference technique to measure film thickness as a function of time. Assuming unit sticking coefficient, the incident flux could be estimated. Typically the flux used was 10^{14} molecules $\text{cm}^{-2} \text{sec}^{-1}$, which corresponds to an effective pressure of about 10^{-7} Torr. This vapor flux was chosen to keep the hydrocarbon vapor pressure at the crystal face much larger than the background pressure and still allow con-

venient growth rates. The crystal was exposed to hydrocarbon vapor either continuously or in doses.

The crystal was heated by passing half-wave rectified current through it. The LEED pattern was viewed during the half cycle when no current was flowing and the pattern was observed continuously during exposure while the temperature was varied. Crystal temperature was measured with a chromel-alumel thermocouple spot-welded to the back of the crystal.

Because of the extreme sensitivity of condensed films of saturated hydrocarbons to electron bombardment, electron beam exposure had to be kept to a minimum. Photographs of the diffraction patterns could only be obtained by using a camera with a fast lens and fast film. The camera used was a Canon Camera Co. Model 7 35 mm with a 50 mm $f/0.95$ lens. Eastman Kodak Tri-X film processed in Acufine photographic developer to give a speed of ASA 1600 was used. Photographic exposures were typically 5 sec at $f/0.95$. Electron beam flux was 5×10^{-5} amp cm^{-2} .

The hydrocarbons employed as adsorbates were all obtained commercially. The *n*-octane, *n*-heptane and cyclohexane were Matheson, Coleman, and Bell Spectro-quality, stated to be of greater than 99% purity. The *n*-hexane was "Baker Analyzed" grade purchased from J. T. Baker Chemical Co. and stated to be of greater than 99% purity. The *n*-butane and propane were Matheson Gas Products Instrument grade, stated to be 99.5% pure. The ethane and methane were Matheson Gas Products ultrahigh purity, stated to be 99.97% pure. The *n*-pentane, *n*-hexane, cyclohexane, *n*-heptane, and *n*-octane were all degassed prior to use by repeated freeze, thaw and pump cycles. The *n*-butane, propane, ethane, and methane were used as supplied by the manufacturer.

RESULTS

First, details of the experimental results for adsorbed monolayers of paraffins are presented, then the results obtained for condensed multilayers are described. The adsorption and growth of cyclohexane are discussed next and finally some observations that apply to both the paraffins and cyclohexane are presented.

LEED observations from monolayers and multilayers of the paraffins and cyclohexane on the (111) crystal face of Pt are strikingly similar, and show similar dependence upon substrate temperature. The heats of adsorption of the paraffins and cyclohexane on Pt(111) are higher than the heats of sublimation of the organic substances. As a result of the stronger substrate-adsorbate bond, monolayers of hydrocarbons condense readily at temperatures where multilayer growth is inhibited. Thus, at constant hydrocarbon pressure, LEED shows no hydrocarbon structure at high temperature; however, at lower temperatures, monolayer structures may be seen. Multilayers are formed at even lower temperatures because the rate of evaporation of the hydrocarbon has fallen below the rate of incorporation of molecules into the film. All of the molecules studied show this behavior.

To facilitate discussion of the *n*-paraffin adsorption



FIG. 1. LEED pattern of one-dimensionally ordered structure of monolayers of the *n*-paraffins on Pt(111). (42 V incident beam).

and growth behavior, three transition temperatures will be defined. These temperatures are different for each paraffin but correspond to identical phenomena.

The highest temperature at which the paraffin monolayer condenses and forms a structure that exhibits only *one-dimensional order* is designated as T_1 . As the temperature is lowered, these monolayer structures become more ordered and form a *two-dimensional surface structure* at T_2 . Upon further lowering of the temperature to T_3 , the rate of condensation of the organic vapor on the surface becomes greater than the rate of evaporation under our conditions of low vapor flux (10^{14} molecules/ cm^2 sec). At this temperature or below, the growth of organic multilayers (crystals) commences. Table I lists these temperatures for each paraffin.

(a) *n*-Paraffins—monolayer adsorption

Exposure of the clean Pt(111) surface to the vapor of the normal paraffins C_5 – C_8 for ~ 10 sec at a pressure of 10^{-7} Torr with the Pt substrate below T_1 produces new diffraction features. These are streaks midway between adjacent Pt(111) first-order diffraction beams and directed perpendicular to the line between adjacent Pt diffraction beams. The streaked pattern is shown in Fig. 1.

With longer exposure, about 20 sec at 10^{-7} Torr, and at temperatures below T_2 , the streaked pattern transforms into a sharp, bright pattern. This pattern is different for each paraffin, but each consists of rows of closely spaced spots replacing the streaks. The diffraction patterns are shown in Figs. 2(a), 3(a), 4(a) and 5(a). Schematic drawings of these patterns are shown in Figs. 2(b), 3(b), 4(b) and 5(b), with only one orientation of the unit mesh illustrated.

Adsorbate surface unit meshes can be defined with

TABLE I. Surface structures and behavior of saturated molecules on Pt(111).

Molecule	$T_1(K)$	$T_2(K)$	$T_3(K)$	Monolayer structures	Multilayer structures
<i>n</i> -Octane	240	220	160	$\begin{vmatrix} 2 & 1 \\ \bar{1} & 4 \end{vmatrix}$	$4.8 \times 12.7 \text{ \AA}$ $\gamma = 79^\circ$ $4.8 \times 4.2 \text{ \AA}$ $\gamma = 105^\circ - [\text{triclinic}(001)]$
<i>n</i> -Heptane	230	215	150	$\begin{vmatrix} 2 & 1 \\ 0 & 8 \end{vmatrix}$	$4.8 \times 11.4 \text{ \AA}$ $\gamma = 78^\circ$ $4.8 \times 4.2 \text{ \AA}$ $\gamma = 105^\circ - [\text{triclinic}(001)]$
<i>n</i> -Hexane	210	195	140	$\begin{vmatrix} 2 & 1 \\ \bar{1} & 3 \end{vmatrix}$	$4.8 \times 10.0 \text{ \AA}$ $\gamma = 76^\circ$
<i>n</i> -Pentane	195	170	125	$\begin{vmatrix} 2 & 1 \\ 0 & 6 \end{vmatrix}$	$4.8 \times 16.6 \text{ \AA}$ $\gamma = 90^\circ$
<i>n</i> -Butane	160	125	105	I $\begin{vmatrix} 2 & 1 \\ \bar{1} & 2 \end{vmatrix}$ low exposure < 105 K	$12.1 \times 12.1 \text{ \AA}$ $\gamma = 60^\circ$
				II $\begin{vmatrix} 2 & 2 \\ \bar{5} & 5 \end{vmatrix}$ low exposure 105-125 K	
				III $\begin{vmatrix} 3 & \bar{2} \\ 2 & 5 \end{vmatrix}$ high exposure	
Propane	140		
Ethane		
Methane		
Cyclohexane	200*		140	$\begin{vmatrix} 4 & \bar{1} \\ 1 & 5 \end{vmatrix}$	$6.3 \times 6.3 \text{ \AA}$ $\gamma = 60^\circ - [\text{monoclinic}(001)]$

*Two-dimensional order-disorder transition.

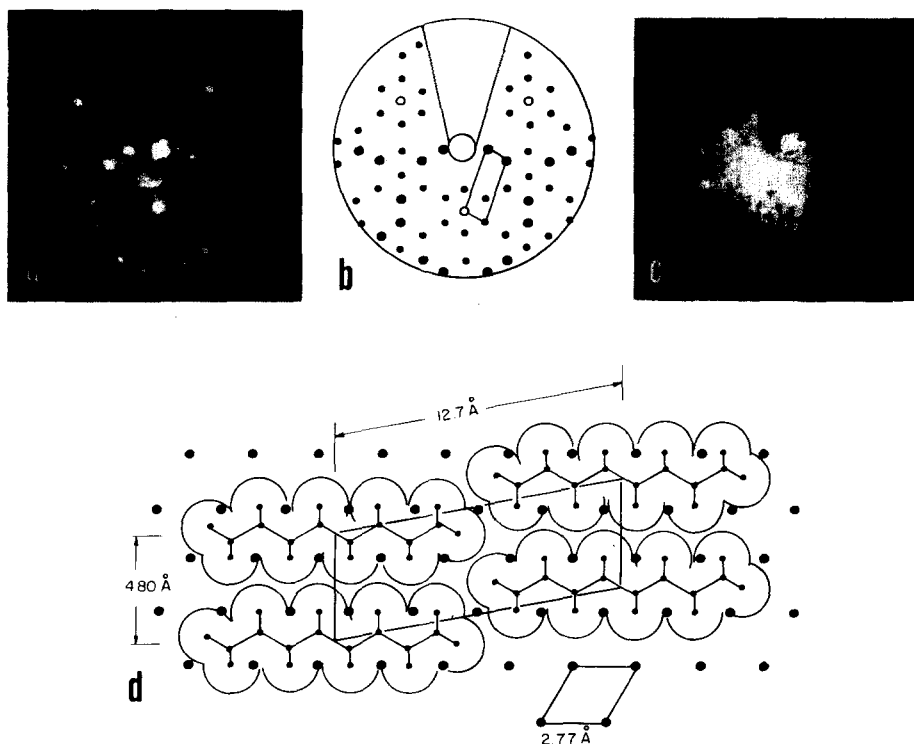


FIG. 2. (a) LEED pattern at 45.5 eV of monolayer of *n*-octane on Pt(111). (b) Schematic drawing of (a) showing one orientation of the primitive reciprocal net. The platinum beams are shown by open circles. (c) LEED pattern at 28.5 eV of a multilayer of *n*-octane grown upon Pt(111). (d) Real space unit mesh of *n*-octane on Pt(111), with proposed arrangement of molecules. Pt atom spacings, bond lengths and van der Waals radii are drawn to scale.

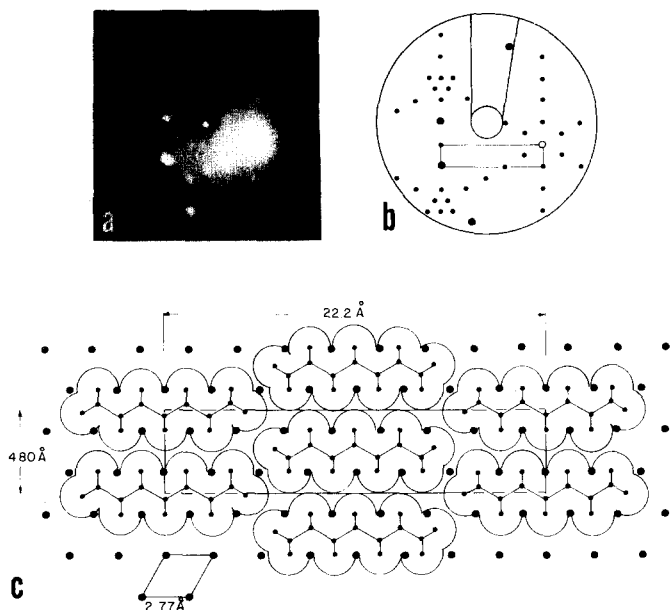


FIG. 3. (a) LEED pattern at 14.2 eV of monolayer of *n*-heptane on Pt(111). (b) Schematic drawing of (a) showing one orientation of the primitive reciprocal net. (c) Real space unit mesh of monolayer of *n*-heptane on Pt(111), with proposed arrangement of molecules.

respect to the substrate unit mesh using a matrix notation.³ If \mathbf{a}_1 and \mathbf{a}_2 are substrate mesh vectors, the adsorbate mesh vectors can be described as $\mathbf{b}_1 = b_{11}\mathbf{a}_1 + b_{12}\mathbf{a}_2$, $\mathbf{b}_2 = b_{21}\mathbf{a}_1 + b_{22}\mathbf{a}_2$, and the adsorbate structure by

$$\begin{vmatrix} b_{11} & b_{12} \\ b_{21} & b_{22} \end{vmatrix}.$$

Choosing \mathbf{a}_1 and \mathbf{a}_2 to be separated by 120° on the Pt(111)

substrate, the ordered paraffin surface structures are

$$n\text{-octane}, \begin{vmatrix} 2 & 1 \\ 1 & 4 \end{vmatrix}; n\text{-heptane}, \begin{vmatrix} 2 & 1 \\ 0 & 8 \end{vmatrix};$$

$$n\text{-hexane}, \begin{vmatrix} 2 & 1 \\ 1 & 3 \end{vmatrix}; \text{ and } n\text{-pentane}, \begin{vmatrix} 2 & 1 \\ 0 & 6 \end{vmatrix}.$$

The unit meshes for *n*-octane and *n*-hexane are oblique, while the meshes for *n*-heptane and *n*-pentane are rectangular. All of these meshes have in common a vector $\sqrt{3}$ times the Pt interatomic spacing (4.8 \AA), directed parallel to $\langle 11\bar{2} \rangle$. The patterns display sixfold symmetry, so all equivalent domains of paraffin structure are present on the Pt(111) surface.

The patterns do not change with additional exposure at temperatures higher than T_3 . Heating the substrate with the adsorbed paraffin above T_2 in the presence of vapor flux or without, causes the LEED pattern to transform to the streaked pattern observed at low exposures. The streaked pattern is also observed when the clean Pt(111) substrate is exposed to paraffin vapor at temperatures between T_1 and T_2 .

These temperature-induced surface structural transitions are apparently reversible at 10^{-7} Torr. Upon heating the ordered structures the LEED pattern changes to the streaked pattern, and then the Pt(111)(1×1) pattern with moderate background intensity. The higher background intensity is due to paraffins adsorbed in a disordered fashion. Cooling the clean Pt crystal in the vapor flux of the various hydrocarbons reverses these transitions.

The adsorption of *n*-butane on Pt(111) produced results different than those obtained from the previously described longer chain C_5 - C_8 molecules. With exposure of 10 sec at 10^{-7} Torr, in the temperature range 90-

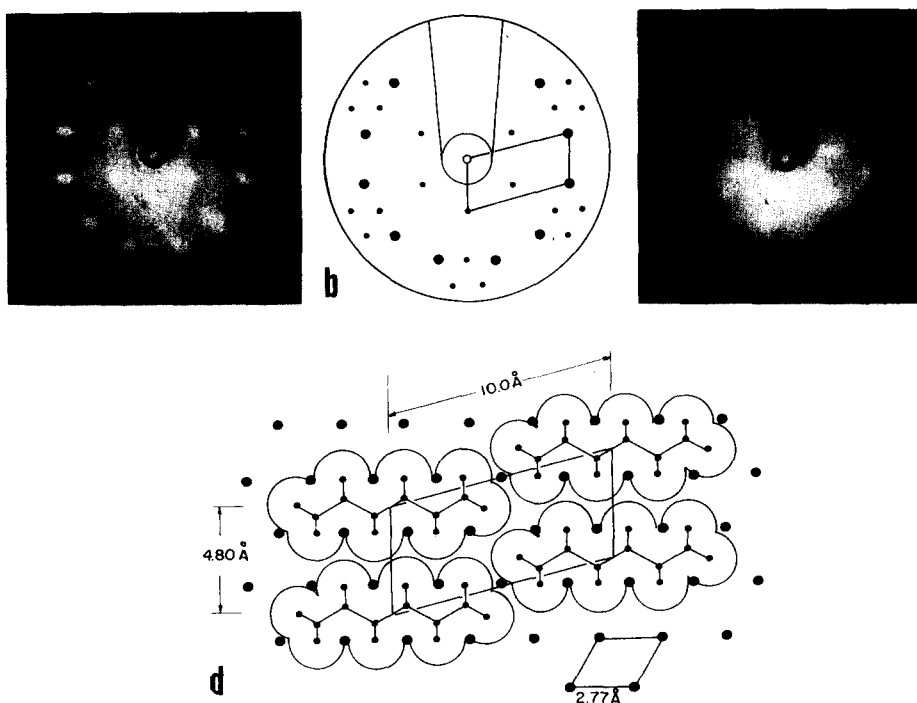


FIG. 4. (a) LEED pattern at 24.8 eV of monolayer of *n*-hexane grown on Pt(111). (b) Schematic drawing of (a) showing one orientation of the primitive reciprocal net. (c) LEED pattern at 24.7 eV of multilayer of *n*-hexane grown upon Pt(111). (0,0) beam is to the right of the electron gun tube. (d) Real space unit mesh of *n*-hexane on Pt(111), with proposed arrangement of molecules.

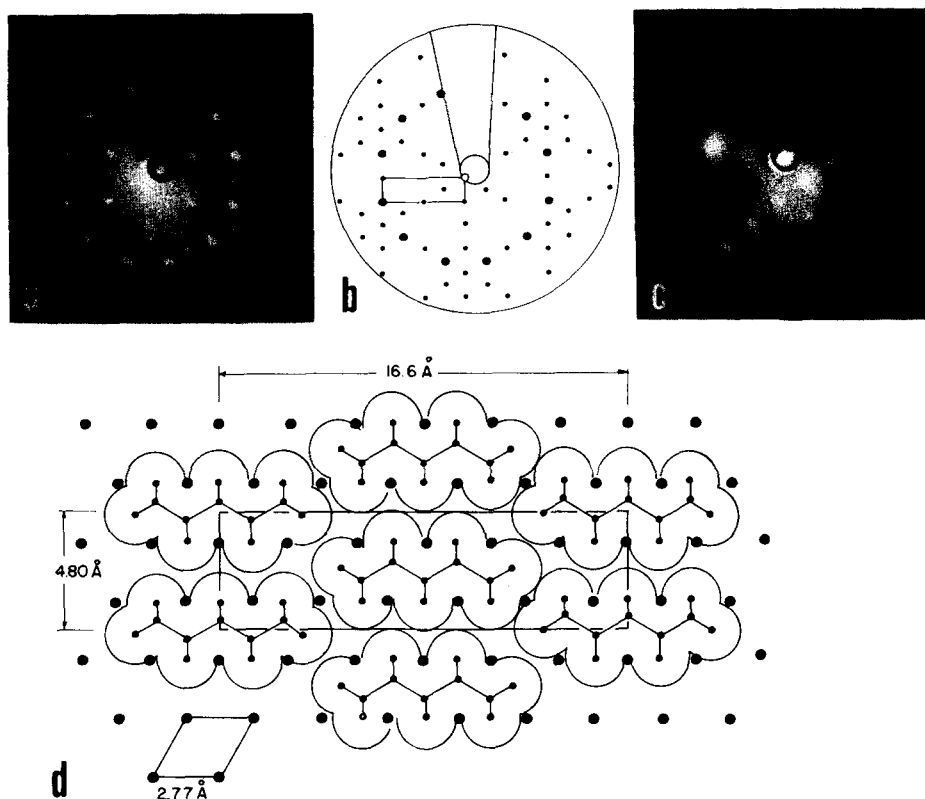


FIG. 5. (a) LEED pattern at 34 eV of monolayer of *n*-pentane on Pt(111). (b) Schematic drawing of (a) showing one orientation of the primitive reciprocal net. (c) LEED pattern at 18.1 eV of a multilayer of *n*-pentane grown upon Pt(111). (d) Real space unit mesh of *n*-pentane on Pt(111) with proposed arrangement of molecules.

105 K, the adsorption of *n*-butane on clean Pt(111) produces the diffraction pattern I shown in Fig. 6(a),

$$\begin{vmatrix} 2 & 1 \\ 1 & 2 \end{vmatrix}.$$

This pattern is quite similar to those observed for *n*-octane and *n*-hexane. Similar exposure of *n*-butane in the higher temperature range 105–125 K produces the diffraction pattern II shown in Fig. 7(a). This pattern

$$\begin{vmatrix} 2 & 2 \\ 5 & 5 \end{vmatrix}$$

is generally not of high quality because it is streaked and the background intensity is moderate at best. This indicates substantial disorder in the structure. The diffraction spots $(h, 0)$ and $(0, k)$ are absent when h or k is odd. Further exposure in the temperature range 90–125 K causes either pattern to transform into pattern III as shown in Fig. 8(a). Pattern III is

$$\begin{vmatrix} 3 & \bar{2} \\ 2 & 5 \end{vmatrix}.$$

The diffraction patterns become streaked and complex during the transformations.

These exposure and temperature-induced structural transformations for *n*-butane also appear to be reversible. The high exposure pattern reverts to the appropriate low exposure pattern if the sample is held in vacuum. Heating the sample above 125 K causes the deterioration of the diffraction features into streaks and subsequent cooling in vacuum results in the reappearance of the appropriate pattern, though of poor quality. Cooling below 125 K in *n*-butane flux restores the high ex-

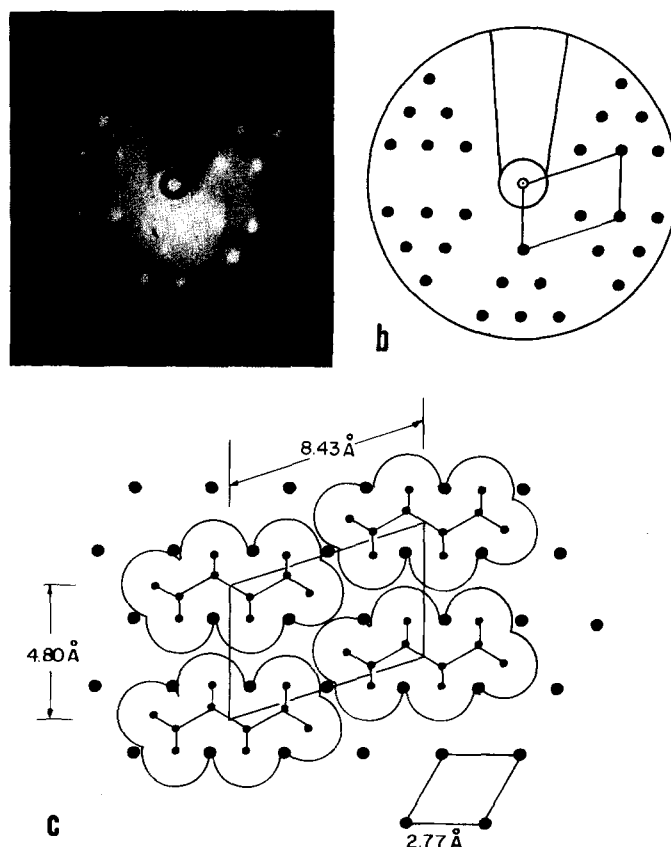


FIG. 6. (a) LEED pattern at 19.5 eV of monolayer of *n*-butane on Pt(111). This structure, designated as I, is seen only below 105 K at low exposure. (b) Schematic drawing of (a) showing one orientation of the primitive reciprocal net. (c) Real space unit mesh of structure I of *n*-butane on Pt(111) with proposed arrangement of molecules.

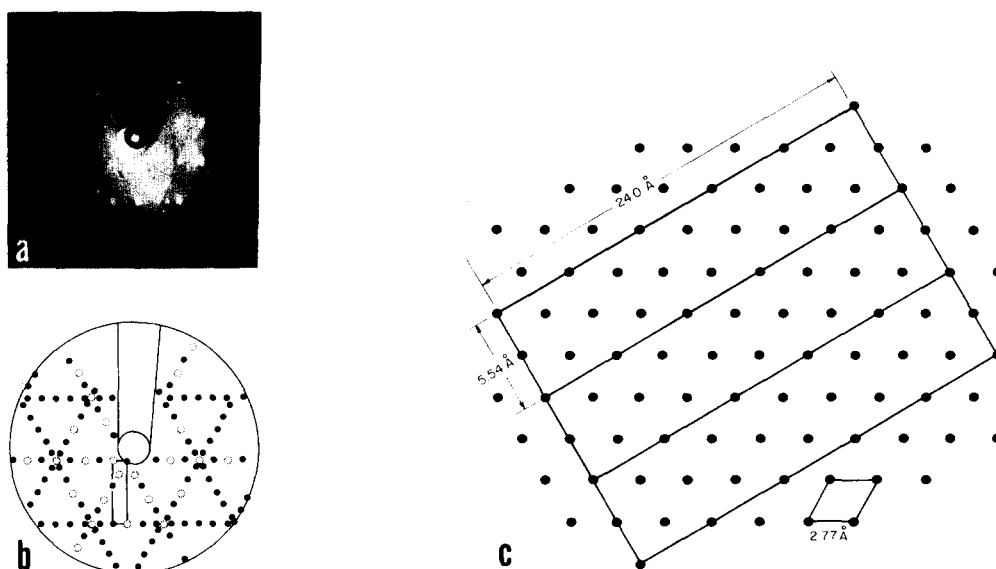


FIG. 7. (a) LEED pattern at 37 eV of monolayer of *n*-butane on Pt(111). This structure, designated as II, is seen only at 105–125 K and at low exposure. (b) Schematic drawing of (a) showing one orientation of the primitive reciprocal net. The unfilled circles indicate systematically absent features. (c) Real space unit mesh of structure II of *n*-butane on Pt(111).

posure pattern III with good quality. This ordering behavior is summarized in Fig. 9.

Exposure of the Pt(111) substrate to the three lightest hydrocarbons, i.e., propane, ethane, and methane, did not produce well-ordered surface structures. Propane adsorption at pressures up to 10^{-5} Torr in the temperature range 90–140 K produced only the streaked pattern

shown in Fig. 1. No new diffraction features were observed at temperatures above 140 K. Exposure of the Pt(111) substrate to methane or ethane at pressures up to 10^{-5} Torr produced no new diffraction features above 90 K.

(b) *n*-Paraffins—multilayers

Exposure of the Pt(111) crystal to the vapors of the normal paraffins C_4 – C_8 at temperatures below T_3 initially yields the ordered monolayer diffraction patterns previously described. Then, with continued exposure, multilayer growth commences and the sharp patterns change. The background intensity increases, the widths of the diffracted beams increase, and the relative intensities of the beams are altered. During this transformation the positions of the beams do not change from their positions in the monolayer patterns. Beam posi-

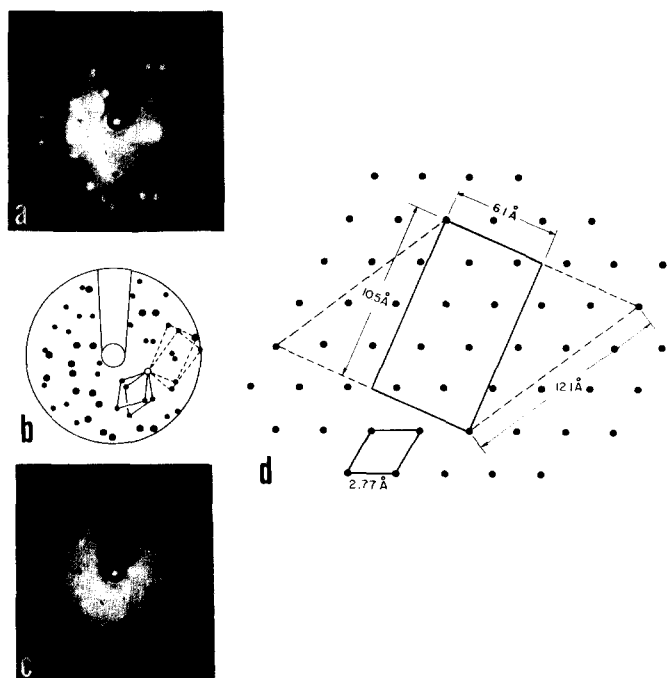


FIG. 8. (a) LEED pattern at 22.2 eV of monolayer of *n*-butane on Pt(111). This structure, designated as III, is seen at high exposures. (b) Schematic drawing of (a) showing two orientations each of two undistinguishable primitive reciprocal nets. (c) LEED pattern at 23.3 eV of a multilayer of *n*-butane grown upon Pt(111). (d) Real space unit mesh of structure III. It is not determined whether the rectangle or the larger rhombus is the correct mesh.

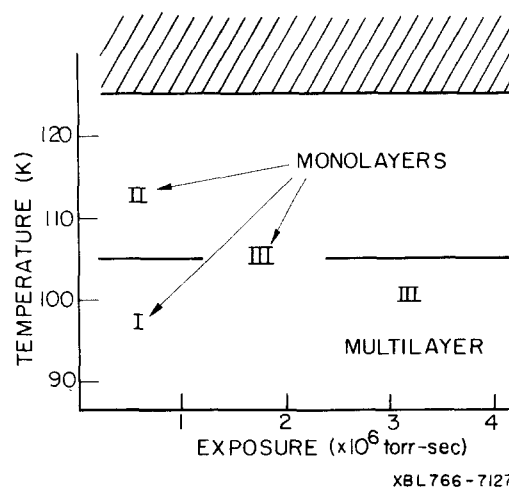


FIG. 9. Diagram showing the *n*-butane structures on Pt(111) and the conditions of temperatures and exposure under which they are observed.

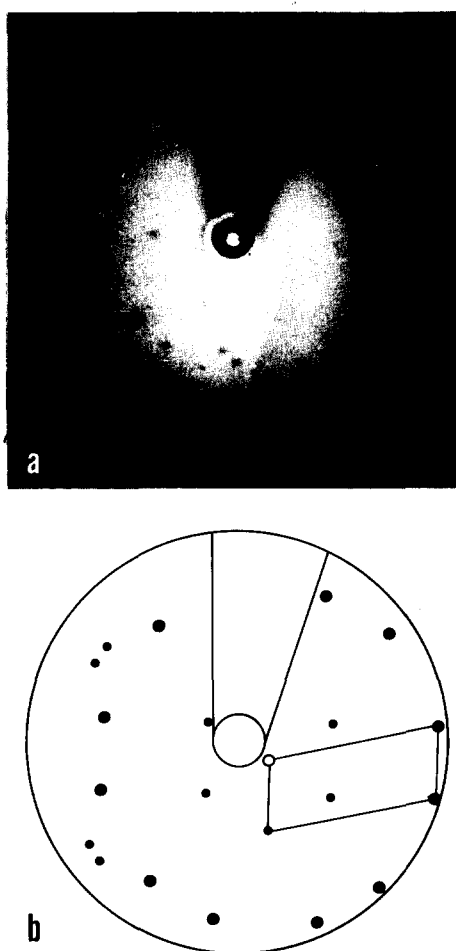


FIG. 10. (a) LEED pattern at 19.2 eV of multilayer of *n*-heptane grown upon Pt(111). (b) Schematic drawing of (a) showing one orientation of the primitive reciprocal net.

tion measurements were accurate to $\pm 5\%$ from thick layers of the paraffins due to the decreased clarity of the diffraction patterns. Simultaneously, the Pt(111) pattern dims and then disappears, becoming visible only at higher incident beam energies. The Pt features are not visible below 250 V incident beam energy when the hydrocarbon layer is estimated to be 50–100 Å thick. Diffraction patterns from thick films of the *n*-paraffins are shown in Figs. 2(c), 4(c), 5(c), 8(c) and 10(a).

This behavior upon thick layer growth is common to all of the paraffins C_4 – C_8 , with two qualifications. The alteration of the intensities of the *n*-heptane diffraction beams causes certain diffraction beams which were already weak for the monolayer to become undetectable for the multilayer. The disappearance of these related beams indicates a change of real space surface mesh to one smaller but related to the *n*-heptane monolayer surface mesh. The *n*-heptane multilayer pattern is shown in Fig. 10. Also, thick layers of *n*-butane grow in the structure of monolayer III, as shown in Fig. 8(c).

If multilayers of *n*-octane or *n*-heptane are condensed upon a disordered paraffin monolayer, or upon the substrate contaminated with ambient gases, other diffraction features are observed. The same pattern, consist-

ing of spots elongated into arcs, is produced by both paraffins and is shown in Fig. 11(a). The pattern is different from either of the previously described patterns. The Pt features are not visible when this pattern is visible. A similar pattern is seen from *n*-hexane, but no new features are seen if *n*-pentane or *n*-butane are condensed upon a disordered monolayer.

Table I lists monolayer and multilayer surface phases observed from adsorption and condensation of each hydrocarbon on Pt(111), along with the temperatures at which the phases are observed. The behavior of the *n*-paraffins at 10^{-7} Torr effective pressure on Pt(111) as a function of temperature is also shown in Fig. 12. The lower curve is the experimentally determined T_3 , the temperature below which a thick film of hydrocarbon may condense at 10^{-7} Torr. The upper curve marks T_2 , the transition temperature from the ordered monolayer phase to the phase exhibiting one-dimensional order giving the LEED pattern shown in Fig. 1. The shaded area is the range of existence of this structure, bound by T_1 . The temperatures are determined to $\pm 5^\circ$ and within these limits there is no change in the range

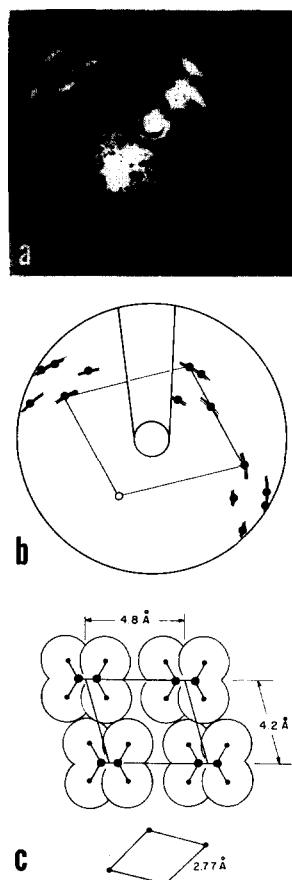
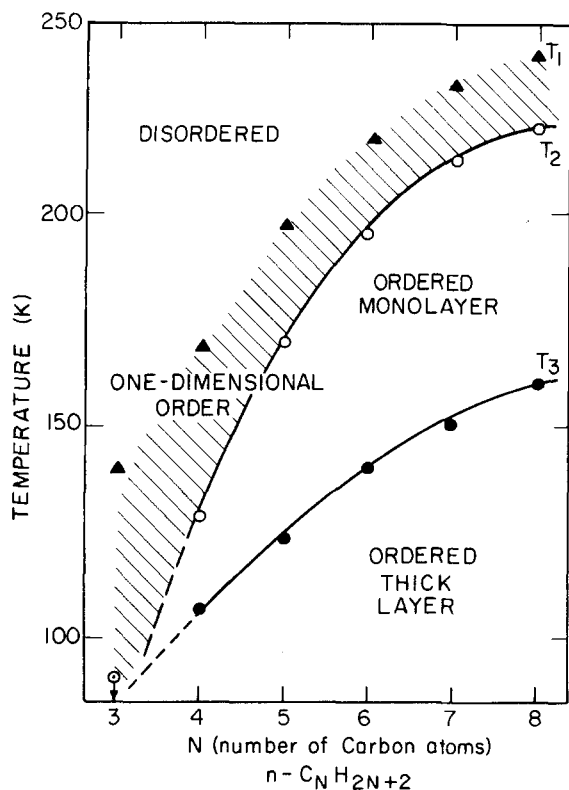


FIG. 11. (a) LEED pattern at 19.4 eV of multilayers of *n*-octane or *n*-heptane grown upon a disordered Pt(111) substrate. (b) Schematic drawing of (a) constructed from the (001) plane of the triclinic paraffin structures, showing one orientation of the primitive reciprocal net. (c) The arrangement of molecules in the (001) planes of *n*-octane or *n*-heptane grown upon the Pt(111) with their orientation with respect to the substrate net approximately as shown.



XBL 765-6794

FIG. 12. Monolayer and multilayer surface phases of the n -paraffins C_3 - C_8 on Pt(111), and the temperatures at which they are observed at 10^{-7} Torr. T_1 , T_2 and T_3 are defined in the text.

of ordering upon changing the paraffin vapor pressure from 10^{-6} to 10^{-8} Torr.

(c) Cyclohexane

Cyclohexane adsorption characteristics on Pt(111) were similar to normal paraffin adsorption. An ordered monolayer structure was observed above 140 K, and an ordered multilayer structure with surface mesh vectors one half as long as the monolayer surface mesh vectors was observed at temperatures below 140 K.

The sharp monolayer pattern is produced by exposure of the clean Pt(111) crystal to cyclohexane vapor at 10^{-7} Torr in the range of 140–200 K. This pattern

$$\begin{vmatrix} 4 & \bar{1} \\ 1 & 5 \end{vmatrix}$$

is shown in Fig. 13(a). Exposure at higher temperature produced no new diffraction features, indicating that cyclohexane does not adsorb in an ordered manner above 200 K at 10^{-7} Torr.

Exposure at temperatures less than 140 K first caused the formation of the monolayer pattern. Continued exposure then produced the multilayer pattern. The multilayer pattern has high background intensity, broader beams, and altered relative beam intensities. The cyclohexane multilayer pattern is shown in Fig. 14(a). The monolayer and multilayer patterns are similar, except that some of the less intense monolayer

features are not visible in the multilayer pattern. In terms of the Pt(111) surface lattice vectors, the multilayer surface net is approximately

$$\begin{vmatrix} 2 & \bar{1} \\ \bar{1} & 5 \end{vmatrix}$$

No patterns were observed upon slow cooling of the sample in cyclohexane vapor flux nor upon exposure of a contaminated Pt(111) surface to cyclohexane vapor.

(d) General observations

The quality of the observed diffraction patterns depends strongly on substrate preparation. The longer the time span after cleaning the crystal and the longer the exposure to the vacuum chamber ambient, the poorer the quality of the diffraction patterns. Well-ordered monolayer structures would be observed only if the hydrocarbons were adsorbed on a clean, cold and well-ordered substrate. The best quality multilayer structures would be observed only if the hydrocarbons were condensed on well-ordered monolayers. The multilayer patterns were of poorer quality than the monolayer patterns and decreased in quality with thickness. The greatest film thickness from which diffraction patterns were detectable was 300 Å. Multilayer diffraction pattern quality was independent of incident vapor flux within the range 10^{12} – 10^{14} molecules $\text{cm}^{-2} \text{sec}^{-1}$, and of sub-

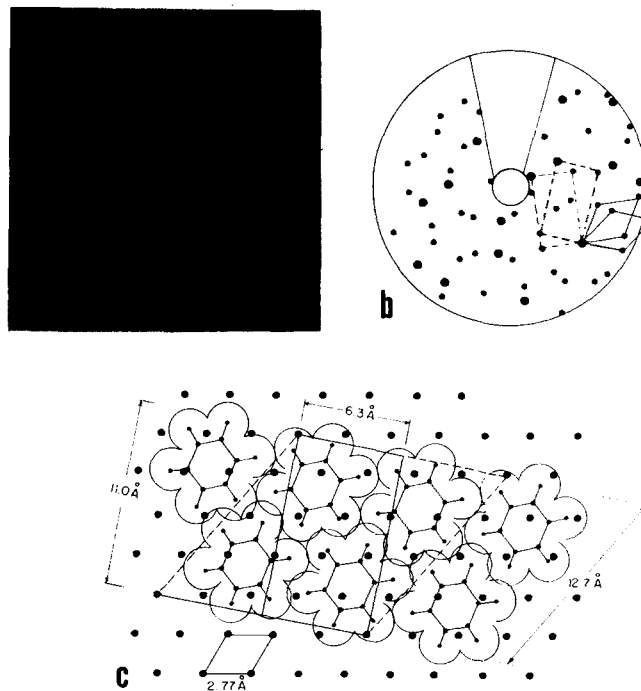


FIG. 13. (a) LEED pattern at 21.2 eV of a monolayer of cyclohexane on Pt(111). (b) Schematic drawing of (a) showing two orientations each of two undistinguishable primitive reciprocal nets. (c) Real space unit meshes of a monolayer of cyclohexane on Pt(111). It is not determined whether the rectangle or the larger rhombus is the correct mesh. Molecules are drawn in the structure of the (001) plane of the cyclohexane crystal structure.

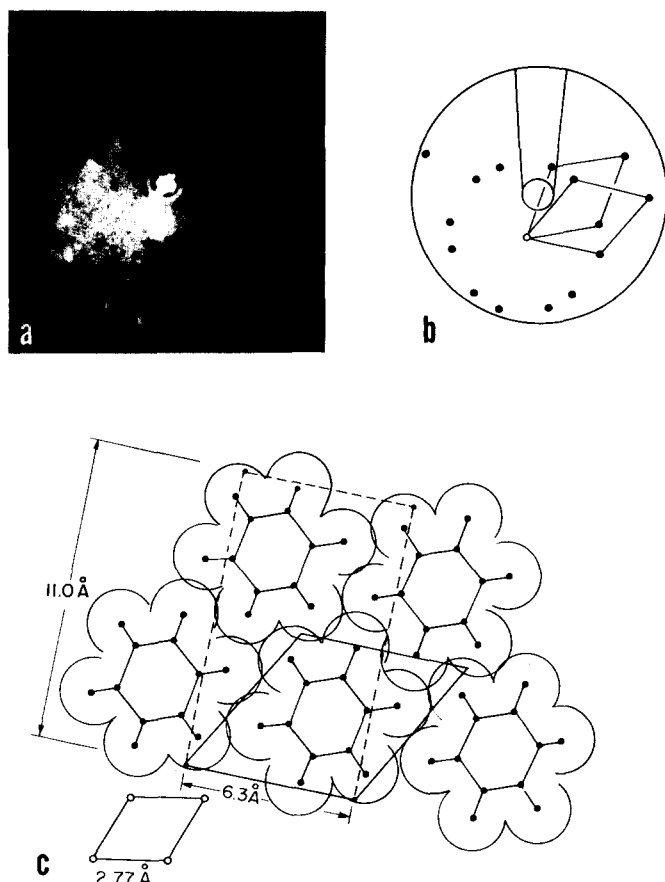


FIG. 14. (a) LEED pattern at 20.2 eV of a multilayer of cyclohexane grown on Pt(111). (b) Schematic drawing of (a) showing two orientations of the primitive reciprocal net. (c) Real space unit mesh of multilayers of cyclohexane grown on Pt(111). The dashed lines show the centered rectangular (001) plane of bulk cyclohexane. The molecules are shown in the structure of the (001) plane of cyclohexane. The orientation of this structure with respect to the Pt substrate is shown.

strate temperature in the range between T_3 and 90 K.

Diffraction features from the monolayer structures were observed from 5–125 V incident beam voltage. In contrast, the multilayer diffraction features were observed only in the range 5–40 V.

The structures produced by condensation of thick layers of these hydrocarbons on Pt(111) were all sensitive to electron irradiation. Typically the pattern would disappear after several seconds of electron exposure at 20 V at 5×10^{-5} amp cm^{-2} . The structures observed at about monolayer coverage would be stable for approximately a minute under the same bombardment conditions. Prolonged beam exposure of either the monolayer or multilayer structures deposits a disordered decomposition product on the Pt crystal surface that obscures the Pt diffraction pattern, does not desorb below 100 °C, and prevents subsequent ordered deposition of hydrocarbon upon it.

Attempts to observe LEED from films of saturated hydrocarbons at greater than 200 Å thickness resulted in the charging of the sample at incident beam voltage less than ~15 V. At a thickness of 300 Å, the surface

would charge below ~20 V. At greater film thicknesses, charging obscured the LEED pattern at even higher beam voltages.

DISCUSSION

n-Paraffins—monolayer structures

The surface unit meshes of monolayers of *n*-butane through *n*-octane on Pt(111) observed in this work are drawn together in Fig. 15. The close relationship between the surface unit cells of the adsorbed *n*-paraffins and between the physical properties of the *n*-paraffins imply that the *n*-paraffins are all in a similar adsorbed state. The smooth variation of unit cell length with chain length at constant width strongly suggest the molecules are adsorbed with the axis of the molecule parallel to the surface. Further, the measured width of the unit cell, 4.80 Å, closely corresponds to the width of the molecule in the plane of the carbon atoms. In the *n*-octane, *n*-heptane and *n*-hexane bulk crystal structures, the width of the paraffin chain is given by the *b* spacings, i. e., 4.79, 4.78 and 4.70 Å, respectively.⁴ The planar all *trans* configuration of the saturated hydrocarbon chain has been found in all determined bulk crystal structures,⁵ and there is evidence that it is found in the liquid *n*-paraffins,⁶ thus it is quite reasonable that these hydrocarbons, bound to the metal

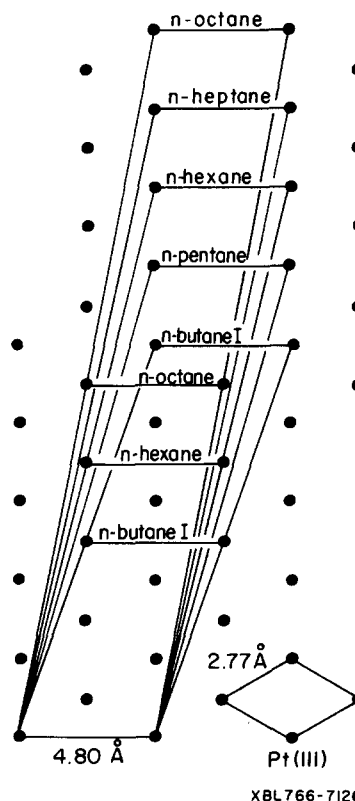


FIG. 15. The observed real space unit meshes of the *n*-paraffins shown with the positions of the Pt atoms in the (111) surface. To emphasize the similarities and trends observed, two unit meshes are drawn for *n*-butane, *n*-hexane and *n*-octane and the meshes of *n*-pentane and *n*-heptane are drawn as oblique parallelograms rather than as the equivalent rectangles shown in Figs. 3 and 5.

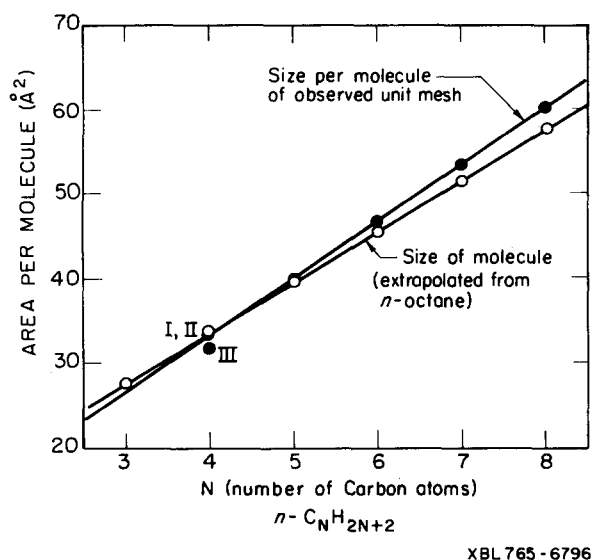


FIG. 16. A plot of the areas per molecule of the observed real space unit meshes of the n -paraffins adsorbed on Pt(111) and an estimate of the area of one cross section of the molecules themselves vs the number of carbon atoms in the n -paraffin. The areas per molecule shown for n -butane structures II and III are based upon an assumed four molecules per unit cell. This figure illustrates the tighter packing of the smaller n -paraffins on the Pt(111) surface.

surface by dispersion forces, are in the same conformation.

The apparent shapes and packing of these molecules in the crystalline solid state are also well known, i. e., $d_{C-C} = 1.54 \text{ \AA}$, $d_{C-H} = 1.08 \text{ \AA}$, $r_H = 1.2 \text{ \AA}$, $\angle CCC = 112^\circ$.⁷ Using this information the molecules can be fit into the observed unit cells with little ambiguity as to relative adsorbate-adsorbate positions, but with less certainty as to relative position of adsorbate and substrate. One could propose surface structures for these adsorbed hydrocarbons assuming the adsorbate position is determined by closest packing of the molecules and surface atoms permitted by van der Waals radii. These proposed surface structures are shown in Figs. 2(d), 3(c), 4(d), 5(d) and 6(c). The structures of the normal hydrocarbons with even numbers of carbon atoms, i. e., octane, hexane and one of the n -butane structures, contain 1 molecule per cell, and the axis of the molecule is parallel to the Pt[110]. The normal hydrocarbons with odd numbers of carbon atoms cannot pack similarly because of crowding of the terminal methyl groups, so they pack with 2 molecules/cell, the two molecules related by a glide plane along [110] with the axis of both molecules parallel to [110]. The proposed glide plane of symmetry in the n -heptane and n -pentane structures should have an effect upon the relative intensities of the LEED spots. The spots (0, k), with k odd, would be forbidden by the glide plane in the proposed structures. The Pt substrate does not share these symmetries, however, and consideration of scattering from the entire structure, adsorbate and substrate, allows finite intensity of these spots.⁸ The spots (0, k) with k odd are noticeably less intense than the other spots in

LEED patterns from n -heptane and n -pentane monolayers supporting the proposed structures.

The n -butane structures II and III [Figs. 7(c) and 8(d)] evidently contain more than one molecule per unit cell. The systematic absences in the structure II diffraction pattern indicate the presence of two mutually perpendicular glide planes, but there are no analogous structures of the other paraffins to support the proposal of a detailed structure. Assuming reasonable packing density with molecules approximately parallel to the surface, one may estimate the number of molecules per cell. For structure I, $z = 1$, the area is 33.2 \AA^2 . For structure II, the area is 133.7 \AA^2 and if $z = 4$, the area/molecule is 33.4 \AA^2 , virtually the same as with the other low exposure structure. The high coverage and thick layer structure, III, has an area of 126.3 \AA^2 . If $z = 4$, the area/molecule is 31.6 \AA^2 , a more dense packing, suggesting that the molecular axis is not parallel to the surface in this structure.

It is significant that n -butane, the smallest of the hydrocarbons showing ordered adsorption in this study, has several structures, with the structure analogous to the larger hydrocarbons stable within only a limited range of temperature and exposure. A plot of monolayer surface unit cell area vs number of carbon atoms of the n -paraffins is shown in Fig. 16. Also plotted is the estimated cross section area of the molecules, estimated by taking the area of n -octane to be the area of the (101) plane of the n -octane crystal structure,⁴ and subtracting 6.0 \AA^2 , the area of a methylene,⁵ for every carbon atom less than eight. The unit cell size is a constant plus n times one half of the Pt interatomic distance (1.39 \AA), while the molecular area is another constant plus n times the projection of the C-C bond length upon the molecular axis (1.28 \AA). The excess space in the unit cell is the difference between the unit cell size and the molecular size and is $n(1.39 - 1.28) \text{ \AA}$ plus a constant. Thus, the smaller the paraffin, the more densely packed it is on the surface. It is perhaps coincidental that the plots intersect at $n = 4$, but the trend is significant. Evidently the packing becomes too dense for n -butane I, thus structures II and III become possible.

Figure 16 also demonstrates that the larger hydrocarbons are more loosely packed in the monolayer. It suggests that adsorbate-substrate interactions are more important than adsorbate-adsorbate interactions in determining surface structures unless adsorbate-adsorbate repulsion is present. It would be important to adsorb still larger n -paraffins to further explore the trends in surface structure and packing.

The only diffraction pattern observed for propane, Fig. 1, is the same as the patterns observed from the larger paraffins at either too low exposure or temperatures between T_1 and T_2 , and indicates only one-dimensional order on the surface. The streaks are in the position of the brightest features of the observed monolayer patterns and correspond to the 4.8 \AA width of the hydrocarbon molecules. This width is shared by all the n -paraffins. The streaking translates to disorder in the perpendicular direction, the direction of the paraffin

chain axis. As the paraffins octane to butane order when cooled from this structure, propane may order also at temperatures less than 90 K which were unattainable in our experiment.

Methane and ethane exposure above 90 K, and propane exposure above 140 K produced no new diffraction features and no appreciable increase in background intensity of the Pt(111)(1×1) pattern. This indicates that under these conditions, methane, ethane, and propane do not adsorb in an ordered fashion, and no more than a small fraction of a monolayer is adsorbed.

The various phase transition temperatures of the adsorbed paraffins, illustrated in Fig. 12, fall on smooth curves, when plotted against paraffin chain length. The T_3 curve agrees reasonably with liquid phase vapor pressure-temperature relationships⁹ extrapolated to low pressures.

T_2 is the temperature of a set of related one-dimensional-two-dimensional order transitions of a number of similar molecules. The LEED data shows that for each molecule both states involved in the transition are similar to the corresponding states in the other paraffins. The entropy of the transitions of all of the molecules may then be expected to be the same. If the enthalpy change of the transition is proportional to the heat of vaporization of the paraffins, and if the entropy changes of all of the molecules are the same, the ratio $\Delta H(\text{vaporization})/T_2$ would be a constant for all of the molecules. The ratio is constant, 37 ± 2 e. u. for the paraffins C_4-C_8 , in support of these assumptions.⁹

The transition at T_1 from the one-dimensionally ordered state to the disordered state showing only the Pt(1×1) LEED pattern may be accompanied by the partial desorption of the paraffin molecules.

n-Paraffins—multilayers

The LEED patterns show that for each normal paraffin the surface unit mesh does not change during growth from an ordered monolayer to the multilayer. The relative beam intensities change, and the overall pattern shows significant disorder in the surface structure, but throughout the growth, the surface mesh stays constant, implying arrangement of molecules at the surface similar to that in the monolayer.

The surface mesh observed from thin and thick films of *n*-octane can be identified with a low index plane of the bulk *n*-octane structure, the (10 $\bar{1}$).⁴ The widths and angles of the two meshes are within 0.5%, and the length of the surface mesh is 4% longer than the bulk mesh. Further, the plane of the *n*-octane molecule is parallel to this plane, as in the proposed monolayer structure. The same surface unit mesh reported here has been observed from multilayers of *n*-octane condensed on Ag(111) over a monolayer structure with a different unit mesh.¹⁰ The growth of multilayers of *n*-octane having the same surface net on two different substrates implies that the surface net is characteristic of the molecular crystal itself and supports the identification of the *n*-octane multilayer surface net with that of

the *n*-octane (10 $\bar{1}$) plane. The surface structure observed from multilayers of *n*-octane is probably an unreconstructed low index plane of the reported *n*-octane crystal structure.

The surface meshes of the other paraffins do not have any obvious relation to the reported crystal structures. The *n*-heptane mesh is rectangular, but the *n*-heptane crystal structure is triclinic. The *n*-hexane crystal structure is very similar to the *n*-octane crystal structure, but the observed surface mesh is significantly different from the (10 $\bar{1}$) plane in which the *n*-hexane molecules lie. The *n*-pentane structure is orthorhombic, with four molecules with nonparallel axes per unit cell and no crystal structure has been reported for *n*-butane.

An explanation for the occurrence of surface structures not related to the reported bulk structures is that the paraffin films grown in these studies are not in the reported bulk crystal structures. There have been eight hydrocarbon chain packing arrangements described from single crystal structure determinations in the literature¹¹ and frequent instances of polymorphism, i. e., multiple bulk crystal structures of a given paraffin.⁵ Evidently no one chain packing arrangement is greatly favored. The presence of an arrangement in the monolayer determined by the Pt(111) substrate causes the subsequent layers to assume the same arrangement, even though that is not the structure favored in the absence of the Pt substrate. Application of a bulk sensitive diffraction technique could test this hypothesis. An alternate explanation, reconstruction of the paraffin surface, is unlikely because the surface unit mesh is the same in the monolayer as it is in the thick layer.

The diffraction pattern from multilayers of *n*-heptane is somewhat different from the *n*-heptane monolayer pattern. Alternate beams of the monolayer pattern are not observable in the multilayer pattern. In the thick layer the unit mesh area of the monolayer is halved by centering the rectangular monolayer mesh. In this way the multilayer surface mesh contains one molecule per unit cell.

The LEED patterns produced by slowly cooling the Pt(111) crystal in *n*-octane or *n*-heptane vapor flux to be below T_3 [Fig. 11(a)] are the same for multilayers of both molecules. The dimensions shared by *n*-octane and *n*-heptane molecules are the cross section of the molecules. In the bulk crystal structures, the cross sections of the molecules are given by the *a* and *b* lattice vectors, and γ , the angle between them. In *n*-octane, $a = 4.22 \text{ \AA}$, $b = 4.79 \text{ \AA}$, $\gamma = 105.8^\circ$; in *n*-heptane, $a = 4.18$, $b = 4.78$ and $\gamma = 105.4^\circ$.⁴ A diffraction pattern constructed from these real space dimensions present in six equivalent azimuthal orientations with the paraffin [100] approximately parallel to the Pt(1 $\bar{1}$ 0) is compared to the LEED pattern in Fig. 11(b). The constructed pattern is entirely consistent with the observed pattern. It is probable that this diffraction pattern is due to unreconstructed (001) planes of the normal crystal structures of *n*-heptane and *n*-octane [Fig. 11(c)]. It is reasonable that this structure was not observed in the smaller paraffins, which share the cross sectional

dimensions of *n*-octane and *n*-heptane. Structures with parallel paraffin chain packing are less favorable for the shorter *n*-paraffins, because of a proportionally larger contribution of end group packing to the lattice energy. In the *n*-pentane crystal structure, neighboring molecules do not have chain axes parallel.

Cyclohexane

The diffraction pattern obtained from monolayers of cyclohexane between 140 and 200 K can be interpreted in two ways, i. e., either as a hexagonal mesh of side 12.7 Å or as a rectangular mesh with lattice vectors of 6.4 Å and 11.0 Å. Both meshes would give identical LEED beam positions. The rectangular mesh dimensions are within 2% of the centered, rectangular *ab* plane of the monoclinic cyclohexane bulk structure stable at these temperatures.¹²

When a thick layer is condensed upon this monolayer structure, certain of the weak diffraction beams disappear. The disappearance of these beams indicates that the rectangular cell has been centered. The thick layer mesh is either the same size and shape as the mesh in the centered *ab* plane of cyclohexane grown with the cyclohexane [010] parallel to the Pt($\bar{1}\bar{4}5$) or, again, because of alternate interpretations of the LEED pattern, half as large. In the bulk structure the planes of the cyclohexane molecules lie almost parallel to the *ab* plane in the chair conformation.

It appears that the thick layer surface structure is the unreconstructed *ab* or (001) plane. The closely related monolayer structure probably is a similar arrangement of molecules with the molecular plane approximately parallel to the Pt surface, but the interaction with Pt(111) surface makes molecules inequivalent that are equivalent scatterers in the bulk structure. There are two possible causes for the inequivalence, actual different orientations of the molecules caused by the inequivalent underlying Pt structure or multiple scattering from the inequivalent underlying Pt structure. It is also unresolved whether the true monolayer surface unit mesh is rectangular, with two molecules/mesh or hexagonal with four molecules/mesh. The hexagonal mesh will have all cells in equivalent registry with the Pt while the rectangular mesh will not. The hexagonal cell is therefore more likely. Upon growth of a multilayer of cyclohexane, all molecules in the surface mesh become equivalent.

Growth behavior

Three types of relationships were observed between monolayer structures and the multilayer structures grown upon them. In the first type there is no similarity between the monolayer structure, ordered or even moderately disordered, and the subsequent thick layer growth. Examples of this behavior are the *n*-octane and *n*-heptane films of (001) orientation (Fig. 11) grown upon disordered surfaces and the naphthalene (001) orientation grown upon either a disordered surface or the Pt(111)-(6×6) naphthalene structure.¹ Grown upon the disordered monolayers, each was oriented randomly

about the surface normal. The occurrence of closely packed low index planes of the reported bulk structures and azimuthal disorder indicates that the substrate played a minimal role in determining the subsequent orientation and structure of the thick layer grown upon it. The disordered monolayer screened out both the crystallographic and chemical effects of the substrate, and the bulk film was free to assume its own structure.

The second type of behavior observed was the formation of a monolayer structure similar or identical to a lattice plane of the bulk structure, and growth of the bulk crystal upon it, with the same structure and orientation. Cyclohexane exhibited this behavior on Pt(111). The lattice plane, the monoclinic (001), consists of a layer of cyclohexane molecules with their molecular planes almost parallel to the lattice plane. The dimensions of this plane and the adsorptive bond between cyclohexane and platinum were compatible with monolayer absorption in this structure, and the structure was maintained during multilayer growth.

The third type of relationship between monolayer and multilayer structures is similar to the second type, except the monolayer and multilayer are *not* in the reported bulk crystal structure. The *n*-paraffins C₅-C₇ and the phthalocyanines exhibit this behavior.¹³ When adsorbed upon clean and ordered substrates, the bonding to the substrate is strong, and in a geometry not related to the expected bulk crystal structures. Rather than grow multilayers of the normal crystal structures, the subsequent layers grow in registry with the monolayer and thus form a crystal structure dependent upon the structure of the substrate. For films of sufficiently small thickness, the contribution of the monolayer adsorption energy to the total lattice energy may offset any loss of lattice energy due to the abnormal bulk structure. Growth of multilayers of these molecules on other substrates will result in other bulk structures, as was observed for the phthalocyanines on Cu(111) and Cu(100).¹³ The growth of unusual crystal structures through the influence of an epitaxial substrate has been called "pseudomorphism." A simple theory of the phenomenon has been proposed by van der Merwe.¹⁴

For the *n*-paraffins, cyclohexane and the phthalocyanines, the multilayer ordering was found to be dependent upon the monolayer ordering, and both were adversely affected by disorder in the layers below them. These observations are in agreement with the above description of the multilayer growth behavior. In the second and third classes of behavior, the multilayer structure duplicates the monolayer structure, and disordered multilayers would form on disordered monolayers. Disorder in the monolayer does not prevent growth of the *n*-octane and *n*-heptane (001) structures, or the naphthalene (001) structure.

Electron beam effects

The saturated hydrocarbons observed in this study are susceptible to low-energy electron bombardment induced decomposition. Matsushige and Hamill¹⁵ measured the yields of decomposition products from multilayer films of cyclohexane and *n*-hexane caused by low-

energy electron irradiation under conditions very similar to the conditions of these studies. They found yields of decomposition events per 100 eV of absorbed energy (G values) to be ~ 0.5 for electron energies of 10–20 eV. With decomposition yields of this magnitude, a monolayer of the hydrocarbons would be decomposed in ~ 10 sec under the conditions of our studies (current density = 5×10^{-5} amp cm^{-2}). LEED patterns from multilayers of all of the hydrocarbons observed in this work would disappear after ~ 5 sec of electron beam exposure, in agreement with the results of Matsushige and Hamill.

The previous work on naphthalene showed that the time for disappearance of the naphthalene diffraction pattern would be about 30 sec under the same bombardment conditions.¹ Buchholz and Somorjai observed¹³ no beam damage effects in various phthalocyanine films after several hours of electron beam exposure. Surfaces of solids composed of large conjugated aromatic molecules are more stable under electron beam irradiation than surfaces of smaller conjugated molecules, and surfaces of saturated molecules are even less stable. This hierarchy of stability is observed for the gas and condensed phases of the molecules under higher energy radiation exposure.¹⁶

Thick layers of the hydrocarbons are more susceptible to damage than monolayers as observed here and as previously observed for naphthalene.¹ This can be understood in terms of interactions with the metal, which provides a ready sink for excitation energy in the monolayer species, so that an excited molecule can de-excite before a bond scission occurs. A molecule at the surface of a thick film does not have the de-excitation pathway so it may dissociate.

These unsaturated hydrocarbons exhibited surface charging at lower thicknesses than did naphthalene, at 200 Å, rather than ~ 1500 Å.

CONCLUSIONS

LEED patterns have been obtained from a series of normal paraffins and cyclohexane, both as adsorbed monolayers and as condensed thick films on Pt(111). The paraffins *n*-octane through *n*-butane all adsorb with chain axis parallel to the Pt substrate. A packing argument explains why *n*-butane will also adsorb in two other structures under different experimental conditions. The adsorbed monolayers of each of the paraffins undergo similar two-dimensional order-one-dimensional order transitions. The surfaces of condensed films of the paraffins maintain the monolayer structures by growing into epitaxially controlled pseudomorphic bulk structures or, in the case of *n*-octane, by growing with the *n*-octane ($\bar{1}01$) plane parallel to the surface. *n*-Octane and *n*-heptane were also observed to grow with unreconstructed triclinic (001) planes parallel to the substrate when grown upon a disordered substrate.

Condensed films of cyclohexane grown on Pt(111) with the unreconstructed monoclinic (001) plane parallel to the substrate. Monolayer adsorption of cyclohexane produces a structure which consists of similar arrangement of cyclohexane molecules, that is with the molecular plane approximately parallel to the Pt.

The rate of damage of molecular crystal surfaces by low-energy electrons is greatest for saturated hydrocarbons and less for aromatic molecules. Monolayers of saturated hydrocarbons adsorbed on platinum are more stable under electron bombardment than the surfaces of multilayers.

This study has demonstrated the feasibility of surface structure studies of thin saturated hydrocarbon crystals using low-energy electrons. It has also shown the utility of LEED studies at low temperatures and the correlation of data from a homologous series of molecules.

ACKNOWLEDGMENT

This work was supported by the U. S. Energy Research and Development Administration. L. E. Firment wishes to acknowledge the support of the National Science Foundation through an N. S. F. Energy-Related Graduate Traineeship.

- ¹L. E. Firment and G. A. Somorjai, *Surf. Sci.* **55**, 413 (1976); *J. Chem. Phys.* **63**, 1037 (1975).
- ²L. L. Kesmodel, P. C. Stair, R. C. Baetzold, and G. A. Somorjai, *Phys. Rev. Lett.* **36**, 1316 (1976).
- ³R. L. Park and H. H. Madden, Jr., *Surf. Sci.* **11**, 188 (1968).
- ⁴N. Norman and H. Mathisen, *Acta Chem. Scand.* **26**, 3913 (1972); **21**, 127 (1967); **15**, 1755 (1961).
- ⁵A. I. Kitaigorodsky, *Molecular Crystals and Molecules* (Academic, New York, 1973), pp. 48–62.
- ⁶N. Norman and H. Mathisen, *The Structure of Linear Polymers. Lower n-Hydrocarbons*. Contract No. DA 91-591-EUC-1166, U. S. Dept. of the Army, European Research Office, Oct. 1960, ASTIA Catalog No. AD-246512.
- ⁷A. I. Kitaigorodsky, Ref. 5, p. 1.
- ⁸R. M. Lambert, *Surf. Sci.* **49**, 325 (1975); B. W. Holland and D. P. Woodruff, *ibid.* **36**, 488 (1973).
- ⁹B. J. Zwolinski and R. C. Wilhoit, *Handbook of Vapor Pressures and Heats of Vaporization of Hydrocarbons and Related Compounds*. American Petroleum Institute Project 44 and Thermodynamics Research Center Publication No. 101, College Station, Texas (1971).
- ¹⁰L. E. Firment and G. A. Somorjai (to be published).
- ¹¹E. Segerman, *Acta Crystallogr.* **19**, 789 (1965).
- ¹²R. Kahn, F. Fourme, D. André and M. Renoud, *Acta Crystallogr. Sect. B* **29**, 131 (1973).
- ¹³J. C. Buchholz and G. A. Somorjai, *J. Chem. Phys.* **66**, 573 (1977).
- ¹⁴J. H. van der Merwe, *Discuss. Faraday Soc.* **5**, 201 (1949).
- ¹⁵T. Matsushige and W. H. Hamill, *J. Phys. Chem.* **76**, 1255 (1972).
- ¹⁶A. Chapiro, *Radiation Chemistry of Polymeric Systems* (Wiley, N. Y., 1962), p. 66.